PERGAMON

Journal of Structural Geology 25 (2003) 935–947

JOURNAL OF STRUCTURAL GEOLOGY

www.elsevier.com/locate/jsg

Characterization of tectono-metamorphic events using crystal size distribution (CSD) diagrams. A case study from the Acebuches metabasites (SW Spain)

Manuel Díaz Azpiroz[a,*], Carlos Fernández[b]

[a]*AYESA, Av. Marie Curie s/n. Parque Tecnológico de La Cartuja. 41092 Seville, Spain*
[b]*Dpto. Geodinámica y Paleontología (Universidad de Huelva). Campus de La Rábida, E-21819, Palos de la Frontera, Huelva, Spain*

Received 7 July 2001; received in revised form 10 June 2002; accepted 20 June 2002

Abstract

Crystal size is one of the main characteristics of a metamorphic rock since it is the result of several processes, including prograde metamorphism as well as retrometamorphism and static and dynamic recrystallisation. In this paper crystal size histograms, mean crystal size, crystal size distribution diagrams, mean aspect ratio and proportion of prismatic sections of amphiboles have been used to describe two tectono-metamorphic events that affected the Acebuches metabasites in the southwestern part of the Iberian Massif. The diagrams depicting the crystal size distribution (CSD) of metamorphic rocks show typically a straight segment that reflects the kinetic conditions during prograde metamorphism as well as retrometamorphic and dynamic recrystallisation processes, and a bell-shaped curve formed during the last stages of growth. The geometrical characteristics of the straight lines of CSD diagrams from different samples of the Acebuches metabasites vary consistently with the structural and metamorphic features indicative of the tectono-metamorphic history suffered by these rocks. This suggests that CSD diagrams can be a useful tool of microstructural analysis in metamorphic rocks.

Keywords: Acebuches metabasites; Southern Iberian Shear Zone; Microfabric; Crystal size distribution (CSD) diagrams; Mylonites

1. Introduction

Quantification of crystal size distribution in recrystallised metamorphic rocks is an important step to help unravel their evolution history. For example, crystal size distribution can provide information on nucleation and growth rates and recrystallisation events (e.g. Marsh, 1988). Based on crystal size analysis, different theoretical models of crystal nucleation and growth during metamorphism have been proposed (e.g. Galwey and Jones, 1966; Jones and Galwey, 1966; Jones et al., 1972), and it has been proven that dynamic recrystallisation giving place to mylonites is a key mechanism for crystal size reduction in a ductile shear zone (e.g. Bell and Etheridge, 1973; White et al., 1980; Tullis and Yund, 1985; Michibayasi, 1993; Michibayasi and Masuda, 1993).

Randolph and Larson (1971) developed a quantitative model to analyse crystallisation in chemical engineering known as the crystal size distribution (CSD) theory, which was adapted to geology by Marsh (1988). CSD theory allows the use of crystal size data to obtain quantitative information concerning several petrogenetic processes such as crystal nucleation and growth rates, nucleation density or annealing. These analyses have been carried out mainly in igneous volcanic rocks (Ghiorso, 1987; Cashman and Marsh, 1988; Maaløe et al., 1989; Peterson, 1990; Armienti et al., 1994; Higgins, 1996; Wilhelm and Wörner, 1996). Few CSD analyses have been made up to date on metamorphic rocks (Cashman and Ferry, 1988). In this paper CSD theory is applied to the partly mylonitized Acebuches metabasites of the Aracena metamorphic belt, Southwestern Spain. The main goal of this paper is to gain further insights into the possible application of CSD theory to obtain a better understanding of the deformation and petrologic processes prevailing during the tectonic evolution of metamorphic rocks.

* Corresponding author. Tel.: +34-959-019857; fax: +34-959-019462
Current address: Dpto. de Cienciàs Ambientales, Universidad Pablo de Olavide, Ctra. de Utrera, Km.1, 41013 Seville Spain.
E-mail address: mdiaazp@dex.upo.es (M. Díaz Azpiroz).

0191-8141/03/$ - see front matter © 2002 Published by Elsevier Science Ltd.
PII: S0191-8141(02)00081-0

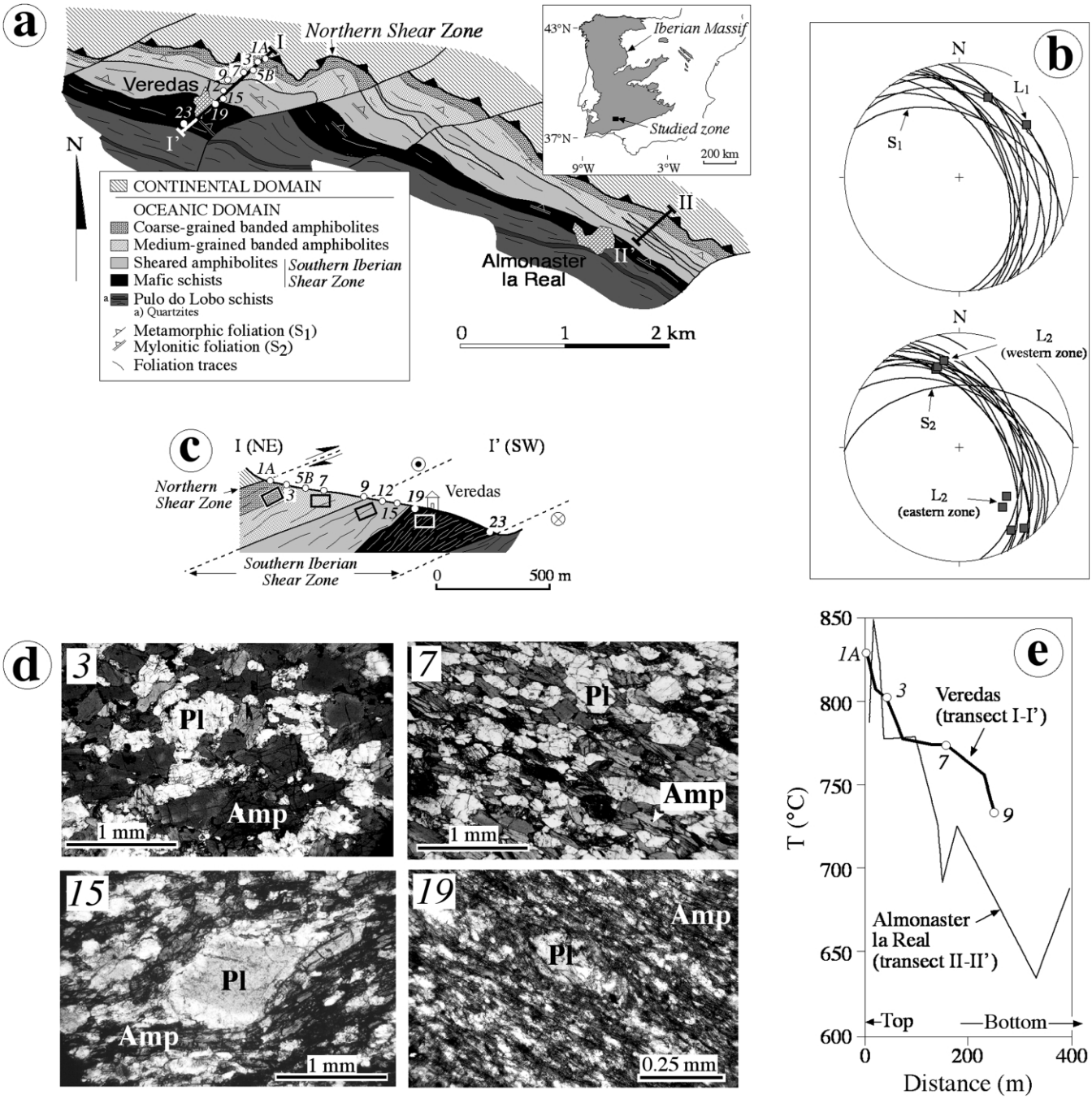

Fig. 1. (a) Geological map of the area of study showing the banded amphibolites and the sheared metabasites (affected by the Southern Iberian Shear Zone). The location of the cross-section and the samples used in this study (1A, 3, 5B, 7, 9, 12, 15, 19 and 23) are also included in the map. The Northern Shear Zone shows essentially an inverse top-to-the-south displacement, as indicated by black triangles. (b) Lower hemisphere equal area projections of structural data from the Acebuches metabasites, including foliation and lineation (S_1 and L_1), as well as mylonitic foliation (S_2) and stretching lineation (L_2). (c) Geological cross-section with the exact location of the samples analysed in this study. Arrows indicate the displacement in the Northern Shear Zone. The left-lateral movement in the Southern Iberian Shear Zone is also marked. (d) Microphotographs illustrating the four lithologic types described in this paper. Mineral symbols are Pl for plagioclase and Amp for amphibole. The approximate location of each photograph is identified as a space in the cross-section. Photographs 3, 7, 15 and 19 correspond to samples studied in this work. (e) Temperature variation in the upper half of the metabasite sheet according to thermometric estimations in two transects of the amphibolite sheet (modified from Díaz Azpiroz, 2001). In transect I–I′ the approximate location of some of the samples analysed in this work (1A, 3, 7 and 9) is also indicated.

2. Geological description of the Acebuches metabasites

2.1. Geologic setting

The Acebuches metabasites are a part of the Aracena metamorphic belt (AMB). The AMB is located at the contact between the Ossa–Morena zone (OMZ) and the South-Portuguese zone (ZSP), two of the main units forming part of the Iberian Massif, located in the south-western part of the European Variscan chain. The AMB is tens of kilometres wide and more than 100 km long, and their limits lie parallel to the main regional structures, which trend in a WNW–ESE direction. According to the division proposed by Castro et al. (1999), two different domains can be distinguished in the AMB: a southern oceanic domain (OD), and a northern continental domain (CD) (Fig. 1). Two groups of rocks are distinguished in the OD. In the northern part, the Acebuches metabasites define a series of amphibolites and mafic schists which, according to geochemical studies, come from a former oceanic crust (Dupuy et al., 1979; Munhá et al., 1986; Quesada et al., 1994; Castro et al., 1996a). To the south of the Acebuches metabasites is located the Pulo do Lobo terrain that has been interpreted by Eden (1991) as a part of a Variscan accretionary prism.

2.2. Structural description

The Acebuches metabasites crop out in a narrow, approximately 1 km wide and more than 100 km long, band. This metabasite sheet is in contact to the north with the CD, and overlies to the south the Pulo do Lobo terrain. The metabasite sheet shows a nearly constant attitude, with a WNW–ESE azimuth and dipping more than 40° to the north. Three main tectono-metamorphic events have been identified in the Acebuches metabasites (Castro et al., 1996a; Díaz Azpiroz, 2001). Firstly, the metabasite sheet was affected by a shear deformation (D_1) accompanied by a high temperature/low pressure (HT/LP) metamorphic event (M_1) that reached the transition between the amphibolite and the granulite facies. This first stage was responsible for the main structures found in the upper structural part of the Acebuches metabasites (Fig. 1a and b). These structures are two penetrative subparallel foliations, a grain size banding and a metamorphic foliation defined by the orientation of amphibole prisms (S_1), and a less penetrative mineral lineation defined by the long axes of amphiboles (L_1). M_1 was more intense at the structural top of the sheet. A parallel increase in the intensity of the deformation associated with D_1 is not clearly observed in the upper half of the amphibolite sheet. The second deformation phase (D_2) was a mylonitization event associated with the development of the Southern Iberian Shear Zone (SISZ) defined by Crespo-Blanc and Orozco (1988). The SISZ is a 200–300-m-thick band, oriented WNW–ESE and dipping more than 45° towards the north (Fig. 1a and b). The main structures associated with D_2 are a penetrative mylonitic foliation (S_2) and a related stretching lineation (L_2). This lineation is defined by the parallel arrangement of linear aggregates of plagioclase and long axes of amphibole crystals. The L_2 lineation shows a low to moderate plunge to the SE in the eastern part of the studied area, and it progressively changes to NW-directed plunges towards the west (Fig. 1b). Sheath and transversal folds, rotated porphyroclasts, $S–C$ and $S–C'$ structures and ultramylonitic shear zones are also found (see Díaz Azpiroz, 2001). Kinematic criteria point to a non-coaxial deformation history for D_2 with a predominant sinistral strike-slip component (Fig. 1c). The mylonitic foliation and lineation are more penetrative towards the structural bottom of the metabasite sheet and the morphology of folds changes in the same sense, which indicates that D_2 was more intense at the structural bottom of the metabasite series and affected only the lowest half of the sheet. The SISZ shows an imbricated structure formed by several shear zones diverging from the main basal one, as it can be appreciated in the map to the east of Almonaster la Real (Fig. 1a). The deformation produced at the SISZ was accompanied by a retrometamorphic event (M_2) that reached the transition between the greenschist and the amphibolite facies. Finally, the third deformation phase (D_3) was related to a metric shear zone, the Northern Shear Zone (NSZ), that developed at the contact between the metabasites and the CD (Fig. 1a and c). Kinematic indicators in the shear zone suggest a predominant top-to-the-south thrust component for the D_3 phase (Fig. 1c).

From the structural top to the bottom of the metabasites, four different facies have been distinguished (Díaz Azpiroz, 2001): coarse-grained banded amphibolites, medium-grained banded amphibolites, sheared amphibolites and mafic schists (Fig. 1). The banded amphibolites show structures due only to D_1 and M_1 whereas the last two facies have been affected by the SISZ. In the sheared amphibolites and mafic schists porphyroclast proportion decreases progressively with increasing distance to the NSZ. Broadly, porphyroclasts represent 10–50% of the rock, so they can be considered mylonites according to the fault rock classification by Sibson (1977). Exceptionally (see, for instance, sample 19 in Fig. 1d), porphyroclasts are less than 10% of the rock (ultramylonites).

2.3. Tectono-metamorphic evolution

Metamorphic conditions for the M_1 event have been constrained by Castro et al. (1996a) and Díaz Azpiroz (2001). These authors analysed selected samples of banded amphibolites, i.e. not affected by the SISZ, using some of the available techniques of amphibole–plagioclase thermometry (Holland and Blundy, 1994) and amphibole thermobarometry (Ernst and Liou, 1998). Pressure estimations are of about 4 kbar (Castro et al., 1996a,b; El-Biad, 2000; El-Hmidi, 2000). The temperature results are summarized in Fig. 1e for two transects located near to the villages of

Veredas (I–I′) and Almonaster la Real (II–II′). A marked increase in temperature towards the top of the amphibolite unit can be seen in both transects. According to structural and cartographic data, Castro et al. (1996a,b) excluded the possibility of a late tectonic inversion of the metamorphic grade in the amphibolite sheet. Therefore, this inversion is considered as an original feature of the M_1 event. The peaks in the temperature curve estimated for the Almonaster la Real transect (Fig. 1e) are a consequence of the stacking associated with the SISZ in this area, which partially repeated the inverted gradient (Fig. 1a). Inverted metamorphic gradients have been profusely documented in subduction-related complexes (e.g. Peacock, 1987). In fact, the OD is considered as a relict of a north-directed subducting slab. In this model, the CD was located at the leading edge of the upper plate. The large temperature gradient in the amphibolite sheet (380 °C/km can be measured in the Veredas transect) has been explained by Castro et al. (1996a,b) as a result of the high temperatures attained in the CD before slab subduction. Castro et al. (1996b) and El-Biad (2000) determined a temperature higher than 900 °C in the southern part of the CD, that may be responsible for the heating of the top of the oceanic slab at the time of subduction.

The M_2 event is a retrograde metamorphism associated with the activity of the SISZ, which produced the classical assemblages with actinolite–chlorite in mafic schists. The data of Fig. 1e come from samples not affected by this retrogression, therefore the inverted metamorphic gradient is independent of the late D_2 shearing.

The tectonic and metamorphic importance of the northern contact of the OD justify why distances within the amphibolite sheet are represented in this paper with respect to the top of the OD. However, it must be remembered that this contact has been affected by the NSZ, which postdates the main episodes of deformation and metamorphism in the OD.

In summary, the available data point to a tectono-metamorphic evolution in two main stages. The older phase (D_1 and M_1) was a shearing event associated with the development of an inverted metamorphic gradient in the amphibolite sheet. This phase was related to the subduction of the OD beneath the CD. The younger episode (D_2 and M_2) was due to the activity of the SISZ that affected the lower half of the amphibolite sheet, associated with a retrograde metamorphism. During this second phase the amphibolite sheet was juxtaposed to the Pulo do Lobo terrain.

3. Methodology

To achieve the quantitative microfabric analysis, nine thin sections of the Acebuches metabasites have been studied. The samples were taken along a transect of the metabasite sheet located near the village of Veredas (Fig. 1a and c, transect I–I′). Samples 1A and 3 correspond to the coarse-grained banded amphibolites. In sample 3 two bands have been studied, a medium-grained band and a coarse-grained band, which have been analysed separately. Three thin sections have been chosen from the medium-grained banded amphibolites (samples 5B, 7 and 9). Samples 12–23 correspond to the SISZ, and vary from sheared amphibolites (12 and 15) to mafic schists (samples 19 and 23).

Thin sections are normal to the foliation plane and parallel to the lineation. Crystal size measurements have been made using a conventional petrographic microscope. The data were collected randomly by point counting, selecting the crystals located in the nodes of a rectangular grid with spacings of 2.2 mm by 1.5 mm. This implies that less than 288 crystals have been analysed per sample (Table 1). In the cases where the same crystal occupied several nodes it was taken as only one measurement. From each crystal the lengths of the long (D) and short (d) axes have been measured. In prismatic and oblique sections of amphiboles D has been determined in a direction parallel to the cleavage planes, with d determined normal to it. D and d directions have been estimated as the lengths of the diagonals in basal rhombic sections of amphiboles. In plagioclase, D and d have been determined in the direction of the cleavage planes. In rounded sections with no cleavage planes the longest and shortest diameters of the crystal have been used instead. Apart from crystal size, the percentage of prismatic sections of amphiboles and the modal proportion of porphyroclasts in samples with a penetrative mylonitic foliation have been computed as well.

We define crystal size (ϕ) as the product between the long and the short axes of each crystal section. As long as we deal with a foliated and lineated fabric, most crystals have a similar orientation and, according to Higgins (1994, 2000), the intersection length statistically corresponds with the real long dimension of the crystal, whereas the intersection width approximates its intermediate dimension. Basal sections of amphibole are normally rhombic and, therefore, the crystal area has been calculated as half of the product between the long and the short axes. Later in this work it will be seen that crystal size histograms have lognormal distributions by number frequency (Jerrall, 2001). Therefore, the mean crystal size (Φ) is obtained as the geometric mean of the individual crystal size observations (e.g. Ranalli, 1984).

The aspect ratio of a crystal ($r_i = D_i/d_i$) is unity when the crystal has a rounded or square shape. The longer the crystal is, the higher the value of the aspect ratio, where D_i and d_i are the length of the long and short axes, respectively, of each crystal section i. The mean aspect ratio (R) of a sample (thin section) is the geometric mean of the aspect ratio measurements.

The crystal population density n is defined as:

$$n(L) = \mathrm{d}N(L)/\mathrm{d}L \quad (1)$$

where $N(L)$ is the cumulative number of crystals per unit

Table 1
Representative statistics of the crystal size distribution of the Acebuches metabasites. Φ is the mean crystal size and S is its standard deviation. N is the number of crystals analysed from each section

		Range (μm^2)	Φ (μm^2)	S ($\mu m^2/n^o$)	Mode (μm^2)	N
MA10971A	Pl	23985000	132103	2637438	51059	117
	Amp	6286875	344273	805648	133333	90
MA10973 (coarse Φ)	Pl	6417980	59580	649800	21818	106
	Amp	9318607	254231	115958	127941	100
MA10973 (medium Φ)	Pl	332380	24996	73285	16818	40
	Amp	747500	102067	167078	47142	81
MA10975B	Pl	321500	20177	39337	7583	165
	Amp	59125	6500	9439	8318	81
MA10977	Pl	205200	20436	30485	14250	101
	Amp	273400	20246	35786	14384	103
MA10979	Pl	360500	25320	44206	12257	131
	Amp	462600	23209	54840	6909	119
MA109712	Pl	143750	5460	20521	3778	79
	Amp	71900	2760	10291	765	105
MA109715	Pl	21050	1520	2779	750	116
	Amp	47950	705	5722	260	96
MA109719	Pl	5675	445	1035	233	94
	Amp	6100	410	777	344	175
MA109723	Pl	1112	136	217	100	45
	Amp	5487	215	878	106	93

volume with long axes equal to or lower than L (Marsh, 1988). Therefore, n is the number of crystals in a given size class and per unit volume. Crystal population density is best represented in a plot of ln(n) against crystal length (L), which is a useful type of CSD diagram (Fig. 2). In order to determine n from the study of thin sections in metamorphic rocks with foliated and lineated fabrics, the crystal intersection length is the most suitable parameter (Higgins, 1994, 2000). To obtain the number of crystals per area in each class-interval of L, the number of crystals with long axes included in a given class has been counted and divided by the total area measured in the thin section. It is possible to transform the population density per unit area to population density per unit volume raising it to the power of 1.5 (Kirkpatrick, 1977). In recent studies, Higgins (1994) and Peterson (1996) have questioned the validity of this approximation, especially in the case of isotropic rocks. Nevertheless, this is not the case for the rocks studied in this work, and the method of Kirkpatrick (1977) could be valid as a simple approximation to the 3-D size distribution. Once the cumulative crystal number per volume is collected, it is divided by the length of the class-interval, and the logarithm of the resulting parameter (n) is represented against L in a CSD diagram (Fig. 2). Crystal size distributions of rocks subjected to regional metamorphism commonly show CSD diagrams with bell-shaped curves (Cashman and Ferry, 1988), with a maximum corresponding to fine-to-medium sizes and a straight line towards coarser crystal size intervals (Fig. 2). For further discussion about CSD diagrams see Shelley (1993) and Marsh (1998).

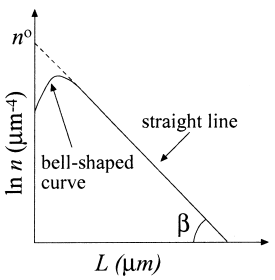

Fig. 2. Graph of crystal population density (n) against crystal length (L). It includes a schematic representation of a typical CSD curve of metamorphic rocks, with a straight segment and a bell-shaped curve. The characteristic parameters of CSDs analysed in this work are the slope (tg β) and the vertical intercept (n^o) of the straight segment. See text for an explanation.

4. Results—crystal size and shape analysis description

4.1. Crystal size histograms and statistics

Frequency plots of crystal size (ϕ) have been represented for the studied thin sections (Fig. 3). Differences in crystal size between samples are very high (see differences in abscissas axes ranges). Therefore, the diagrams are separated into three groups. Crystal size distributions are mostly bell-shaped and show a positive skewness with the geometric mean displaced to the right of the mode. Coarse-grained banded amphibolites (samples 1A and 3) show the largest mode, which decreases abruptly towards medium-grained banded amphibolites (samples 5B, 7 and 9). Here the mode becomes stable or may even increase slightly. This pattern is also clearly depicted in Fig. 3a. The relative proportion of fine crystal sizes increases with the distance from the NSZ, with an abrupt change between samples 9 and 12 (Fig. 3c and d). The statistics obtained from the crystal size measurements (range, mode and

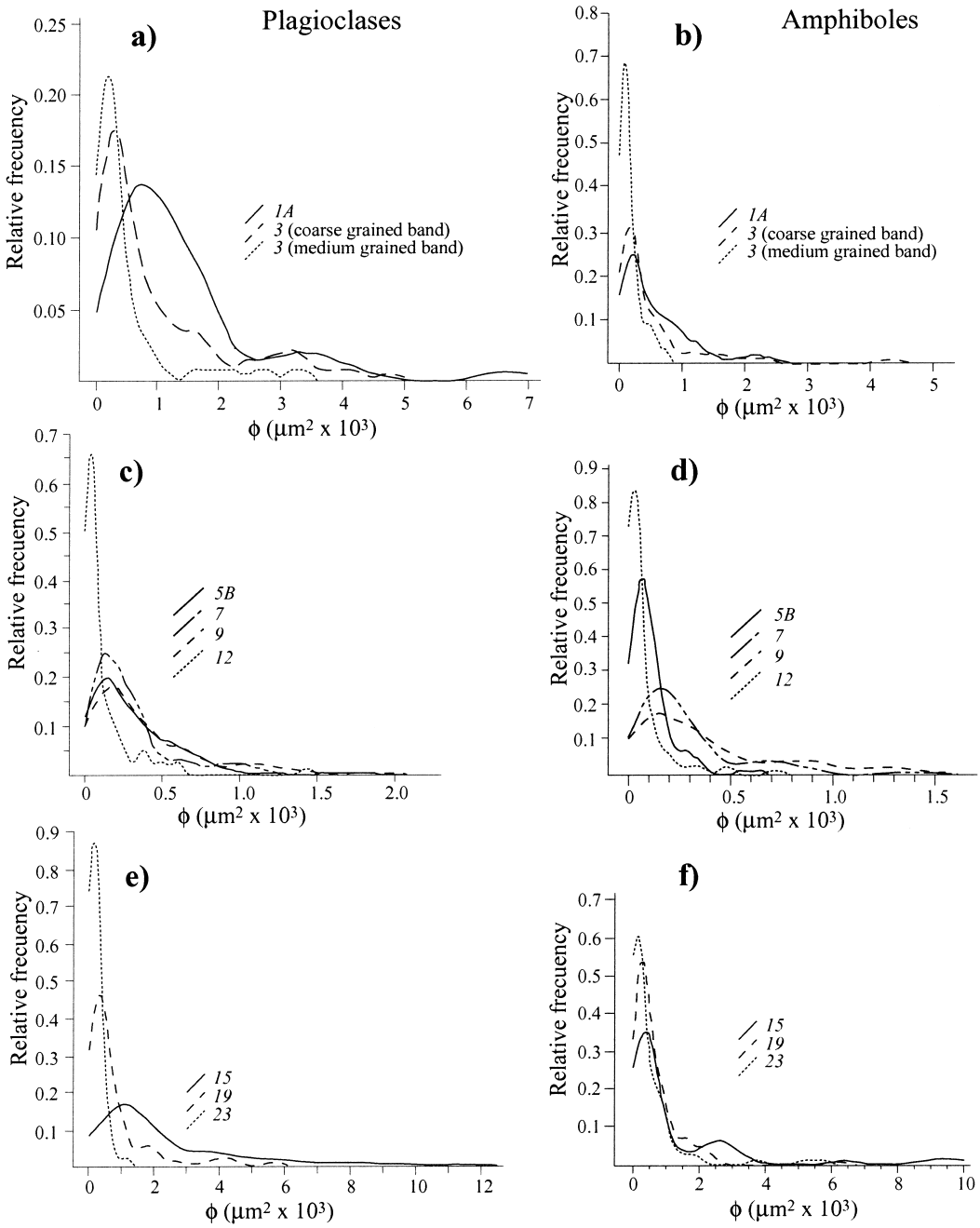

Fig. 3. Crystal size (ϕ) frequency plots. Parts (a) and (d) correspond to samples located at the structural top of the series, (b) and (e) to samples in the middle part and (c) and (f) show samples from the bottom.

geometric mean) are displayed in Table 1, and represented against distance to the structural top of the metabasite sheet (the NSZ) in Fig. 4. Mean crystal size (Φ) decreases rapidly from the coarse-grained banded amphibolites, remains approximately constant in medium-grained banded amphibolites, and suffers a steep drop between samples 9 and 12 (Fig. 4a and b). From the latter towards sample 23, Φ shows an asymptotic decrease reaching a nearly constant value between samples 19 and 23. The crystal size range shows an evolution similar to that of the mode (see Table 1). The wavelength of the curve and the crystal size standard deviation (S) decrease with the distance to the NSZ (Figs. 3 and 4c and d), indicating a trend towards a lower data dispersion.

4.2. Fabric strength

Fabric strength, as defined by Ree (1991), is determined by the shape and orientation of crystals. The evolution of the mean aspect ratio (R) with the distance to the NSZ is shown in Fig. 5a. In banded amphibolites (samples 1A–9), plagioclases have long axes that are approximately 1.5 times longer than the short ones. In the metabasites affected

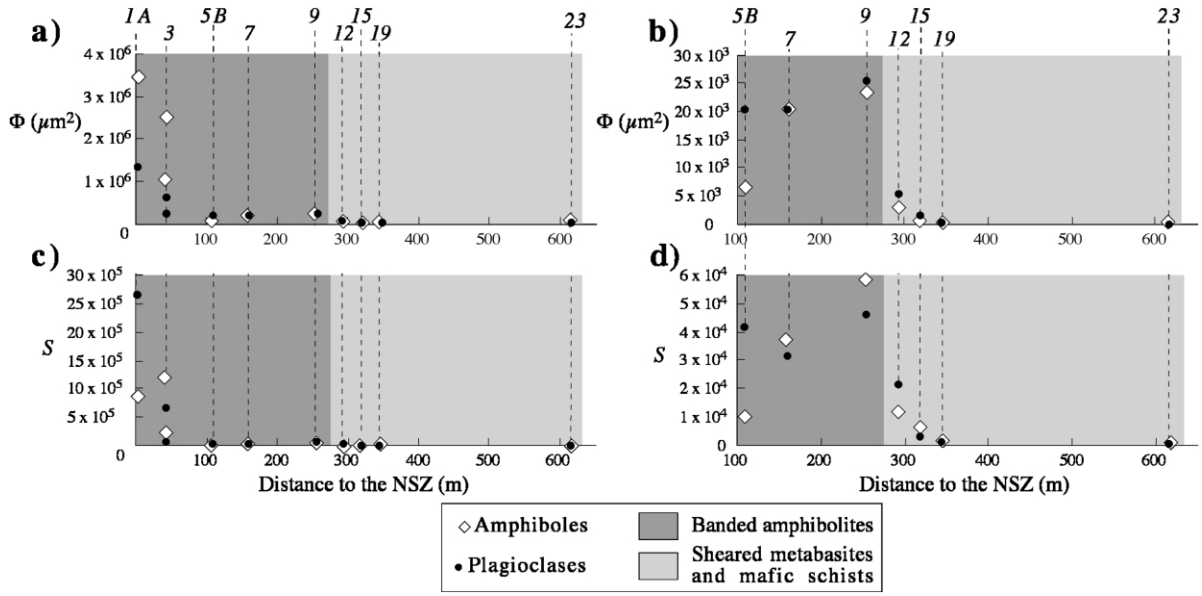

Fig. 4. Evolution with the distance to the Northern Shear Zone (NSZ) of mean crystal size (Φ) and its standard deviation (S). Parts (b) and (d) are an enlargement of scale of (a) and (c), respectively. Italic numbers in each diagram correspond to the different samples.

by the SISZ, the plagioclase crystals are more elongated, being the long axes twice the short axes. Amphiboles show a short prismatic habit ($R = 1.5–2.2$) in banded amphibolites. R increases abruptly from sample 12 towards the bottom of the sheet, reaching values well exceeding three. This change suggests that in sheared metabasites amphiboles have a long prismatic habit, which becomes more pronounced as the distance to the NSZ increases. Another way to estimate the fabric strength is by calculating the proportion of prismatic crystal sections of amphiboles. In rocks with a well developed plano-linear fabric the proportion of prismatic sections found in a thin section normal to the foliation and parallel to the lineation should be high, since basal or oblique sections would correspond to crystals that are misoriented with respect to the fabric. In the Acebuches metabasites, the variation of the proportion of prismatic sections of amphiboles with the distance to the NSZ (Fig. 5b) is similar to the evolution observed for R.

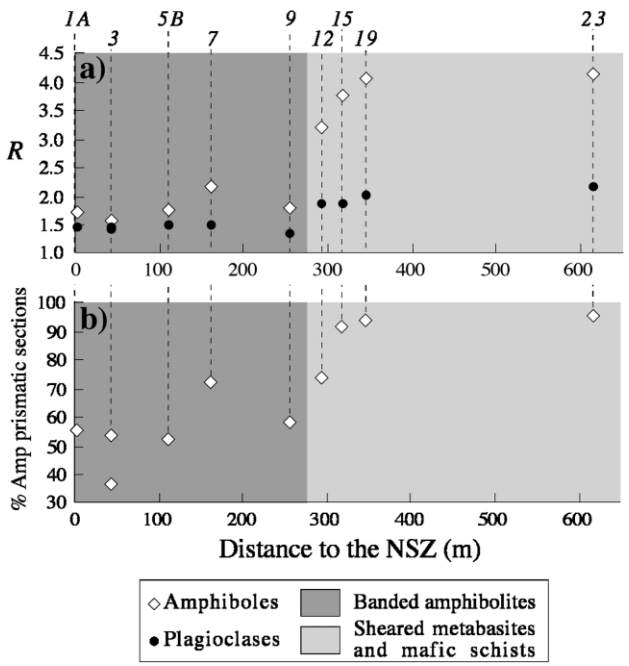

Fig. 5. Evolution with the distance to the Northern Shear Zone (NSZ) of (a) the mean aspect ratio of plagioclases and amphiboles (R), and (b) the proportion of prismatic sections of amphiboles. Italic numbers in each diagram correspond to the different samples.

4.3. Crystal size distribution (CSD) diagrams

CSD diagrams of the Acebuches metabasites show a bell-shaped curve located at fine-to-medium size crystal intervals. This is followed by a straight line with negative slope, which indicates a decrease in population density with increasing grain size (Fig. 6). Although this pattern is similar for all the studied samples the slope of the straight line and its intercept with the vertical axis change from one sample to another. The maximum in the bell-shaped curve reaches higher n values and is displaced towards finer grain size intervals with the distance to the NSZ (Fig. 6). In order to compare the CSD diagrams, the slope (tg β) and intercept with the y-axis (n^{o}) of the straight line have been measured (see Fig. 2 for a definition of these parameters). In samples 9 (medium-grained banded amphibolites) and 19 (mafic schists) the point corresponding to the largest class-interval deviates from the main straight segment of the corresponding CSD diagram. This can be considered as a change in the slope of the straight line (Fig. 6f and i), although the low statistical significance of this second straight segment precludes further interpretations.

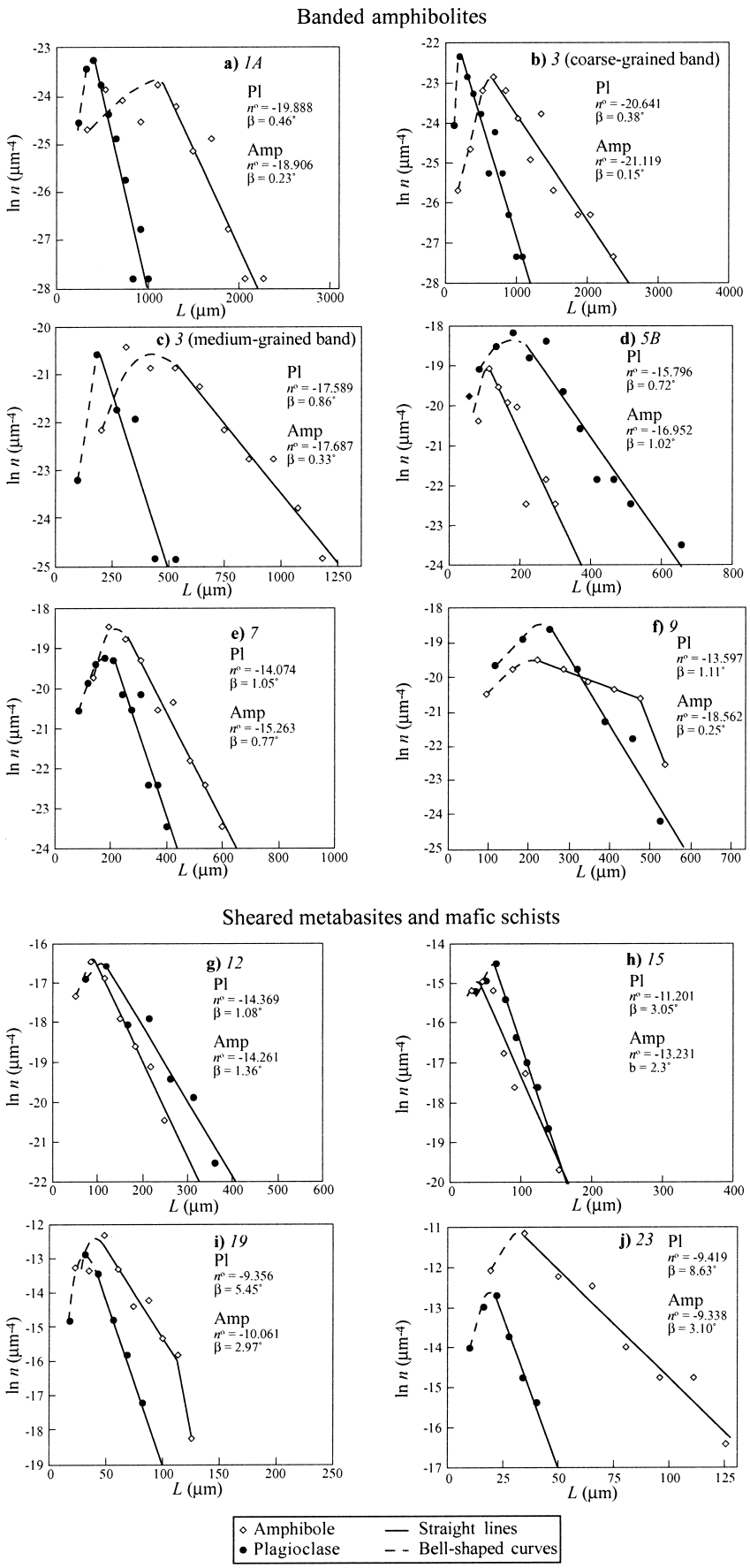
Banded amphibolites
a) 1A
Pl
n° = -19.888
β = 0.46°
Amp
n° = -18.906
β = 0.23°
b) 3 (coarse-grained band)
Pl
n° = -20.641
β = 0.38°
Amp
n° = -21.119
β = 0.15°
c) 3 (medium-grained band)
Pl
n° = -17.589
β = 0.86°
Amp
n° = -17.687
β = 0.33°
d) 5B
Pl
n° = -15.796
β = 0.72°
Amp
n° = -16.952
β = 1.02°
e) 7
Pl
n° = -14.074
β = 1.05°
Amp
n° = -15.263
β = 0.77°
f) 9
Pl
n° = -13.597
β = 1.11°
Amp
n° = -18.562
β = 0.25°
Sheared metabasites and mafic schists
g) 12
Pl
n° = -14.369
β = 1.08°
Amp
n° = -14.261
β = 1.36°
h) 15
Pl
n° = -11.201
β = 3.05°
Amp
n° = -13.231
b = 2.3°
i) 19
Pl
n° = -9.356
β = 5.45°
Amp
n° = -10.061
β = 2.97°
j) 23
Pl
n° = -9.419
β = 8.63°
Amp
n° = -9.338
β = 3.10°
ln n (μm-4)
L (μm)
◇ Amphibole
● Plagioclase
— Straight lines
– – Bell-shaped curves

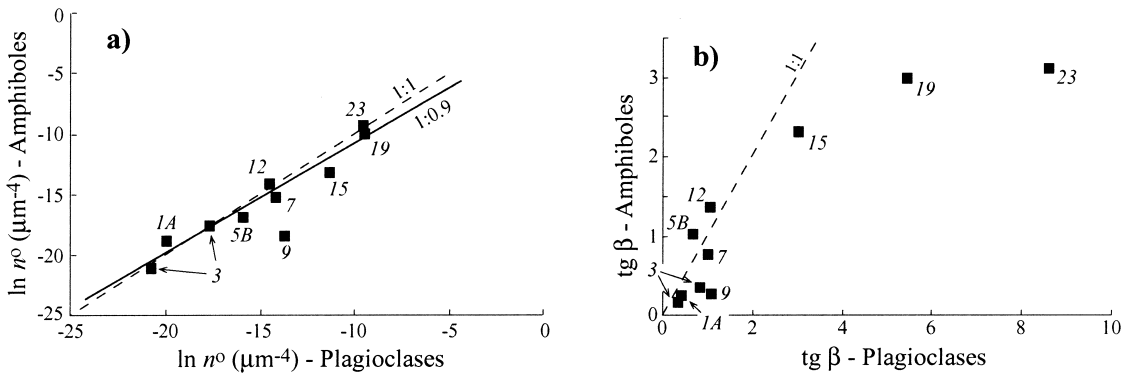

Fig. 7. Comparison of the characteristic parameters that define the straight lines of CSDs of plagioclases and amphiboles. (a) Intercept with the *y*-axis (n^{o}). (b) Slope (tg β). Italic numbers in each diagram correspond to the different samples.

The relationships between the parameters (n^{o} and tg β) describing the straight lines of plagioclases and amphiboles are represented in Fig. 7. The intercept parameter (n^{o}) for plagioclases and amphiboles in the measured samples shows a reasonable fit ($R^2 = 0.83$) to a straight line with a slope close to unity (0.9) (Fig. 7a). However, in most cases, the straight lines of the CSD diagrams of plagioclases have a higher slope than the diagrams corresponding to amphiboles (Fig. 7b).

The slope (tg β) and the intercept (n^{o}) of the straight line in the CSD diagrams show a positive correlation (Fig. 8a and b). Similar results are obtained for plagioclases and amphiboles. However, some differences can be observed between banded amphibolites and sheared metabasites. In this sense, samples 1A–9 show similar values of tg β, while n^{o} increases progressively with the distance to the NSZ (Fig. 8c and d). This suggests that the straight lines of CSD diagrams are displaced towards higher n^{o} values maintaining its slope with increasing distances to the NSZ (Fig. 9a). At the same time, the maximum length of each sample decreases towards the bottom. On the other hand, in samples corresponding to rocks affected by the SISZ (samples 12, 15, 19 and 23) the straight lines show only slight changes in intercept as their slope increases (Fig. 8c and d). This indicates that inside the SISZ (samples 12–23) the straight lines progressively pivot around n^{o} towards a more inclined position (Fig. 9b), which suggests that the coarsest crystal sizes are progressively eliminated.

5. Discussion—crystal size and shape analysis interpretation

5.1. Crystal size histograms and fabric strength

The lognormal distributions of crystal size histograms are typical of metamorphic rocks (Jones and Galwey, 1966; Kretz, 1966; Jones et al., 1972; Cashman and Ferry, 1988; Eberl et al., 1990) and of mylonites that have undergone dynamic recrystallisation (Ranalli, 1984; Michibayasi, 1993; Michibayasi and Masuda, 1993). The variation in the crystal size and shape parameters shown in Figs. 4 and 5 is due to the tectono-metamorphic evolution suffered by the metabasite sheet. In this sense, the inverse metamorphic gradient associated with M_1 is clearly imprinted in the decrease of the mean crystal size from samples 1A–9 (Fig. 4a). The sudden drop in the mean crystal size between samples 9 and 12 (Fig. 4b) and the increase in the mean aspect ratio *R* (Fig. 5a) are a clear consequence of the activity of the SISZ. The metabasites that were affected by the SISZ (samples 12, 15, 19 and 23) show important textural differences with respect to the banded amphibolites. In fact, in the lower half of the series the medium and coarse crystals have disappeared except for a few porphyroclasts (Fig. 3c–f). The fabric strength (the mean aspect ratio *R* and the proportion of prismatic sections of amphiboles; see Fig. 5a and b) becomes higher towards the inner part of the SISZ, which also coincides with the observed increment in the intensity of mylonitic deformation (Díaz Azpiroz, 2001). In the lower levels of the SISZ (samples 19 and 23) both crystal size reduction and fabric strength reached a maximum and remained approximately constant, as it is proven by the asymptotic shape of the mean crystal size, mean aspect ratio and proportion of prismatic sections of amphiboles diagrams (Figs. 4 and 5). This suggests that in the inner part of the SISZ the mylonitic fabric reached a strain-independent steady state in the sense of Means (1981).

5.2. CSD diagrams and tectono-metamorphic events

The variations observed in the CSD diagrams of the Acebuches metabasites are summarized in Fig. 9. Two main sectors have been identified, corresponding to the banded

Fig. 6. CSD diagrams for the studied samples of the Acebuches metabasites. Straight line segments are computed by means of a linear least-squares fit to data for the larger crystals. In each diagram the characteristic parameters of the straight line are shown.

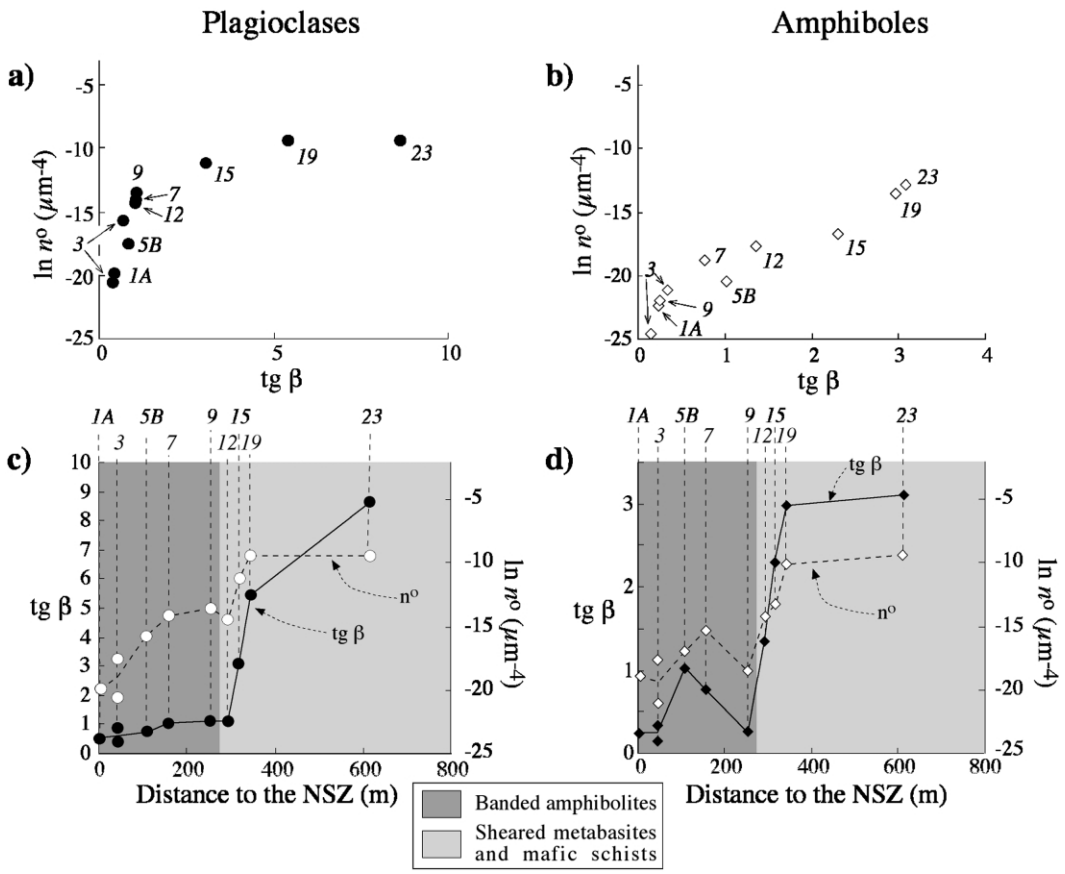

Fig. 8. Relationships between the two characteristic parameters (n° and tg β) of the straight lines of the studied samples for (a) plagioclases and (b) amphiboles. Evolution with the distance to the Northern Shear Zone (NSZ) of the characteristic parameters of (c) plagioclases and (d) amphiboles. Italic numbers in each diagram correspond to the different samples.

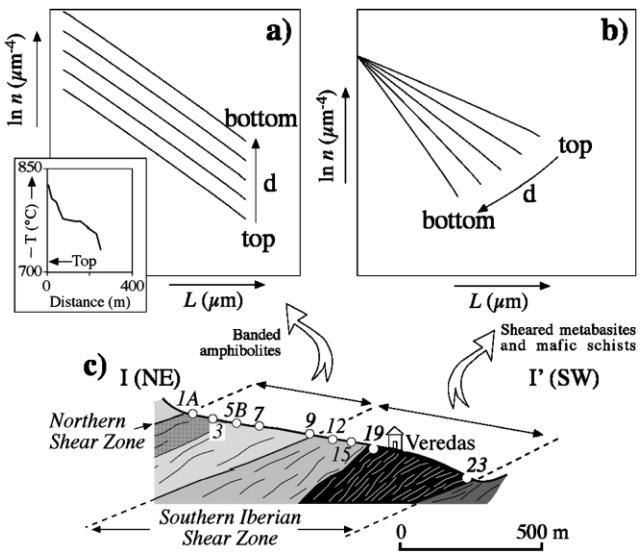

Fig. 9. Schematic evolution of the straight line from CSD diagrams of the Acebuches metabasites as a function of the distance (d) to the Northern Shear Zone (NSZ). (a) Banded amphibolites (samples 1A–9). Inset shows the variation of the estimated metamorphic temperature with distance (see Fig. 1e). (b) Sheared metabasites (samples 12–23). (c) Cross-section (Fig. 1c) with the location of the studied samples and the position of the two sectors with differently evolving CSD diagrams. See the text for further explanation.

amphibolites affected only by D_1 and M_1 (Fig. 9a), and the sheared metabasites that were also affected by the D_2–M_2 event, associated with the activity of the SISZ (Fig. 9b).

The straight lines of the CSD diagrams of the banded amphibolites have a similar slope differing in the intercept, which increase towards the bottom of the banded amphibolites (Fig. 8a–d). According to Marsh (1988), the intercept in CSD diagrams is the nucleation density at the smallest crystal size. It is expected that samples with higher intercept values (i.e. higher nucleation rates) will show finer crystal size. This coincides with the field and microscope observations in the Acebuches banded metabasites (Fig. 1d, samples 3 and 7, and Fig. 4a). The relation shown in Fig. 7a indicates that nucleation densities were almost identical for amphiboles and plagioclases in a given sample. On the other hand, the constant slope suggests that the conditions affecting the growth rate, which is proportional to the slope of the straight line (Marsh, 1988), were essentially the same in the upper half of the series. These variations in the shape of CSD diagrams are parallel to the observed decrease in temperature in the banded amphibolites (Fig. 1e and inset in Fig. 9a) defining the inverted metamorphic gradient of the Acebuches metabasites (Bard, 1969, 1970; Crespo-Blanc, 1991; Castro et al., 1996a; Díaz Azpiroz,

2001). Other sources of variations in the CSD diagrams, like compositional variations or shearing effects, can be excluded in this case. In fact, banded amphibolites are compositionally very homogeneous (Castro et al., 1996a) and were not affected by the SISZ (Díaz Azpiroz, 2001). Therefore, the CSD diagrams seem a very promising tool to describe temperature variations in metamorphic rocks. In the Acebuches case, a temperature decrease of 100 °C (Fig. 1e) implies a correlative increase of around five orders of magnitude in the intercept of the straight line of CSD diagrams (Fig. 8a–d). These observations are valid for both plagioclases and amphiboles, the essential minerals forming the Acebuches amphibolites.

The straight line of the CSD diagrams of the fine grained metabasites have a much higher slope than that of the banded amphibolites (Fig. 8). The sudden change in the slope of the straight lines, which is observed to start between samples 9 and 12 (Fig. 8), coincides with the transition between the banded amphibolites and the sheared metabasites. Downwards from sample 12, the slope ($\mathrm{tg}\,\beta$) increases progressively (Figs. 8b and d and 9b), in parallel with the intensity of the deformation associated with the SISZ as shown by Díaz Azpiroz (2001) based on a number of structural evidences (variations in fold style, foliation and lineation patterns, kinematic criteria, etc.). Again, both plagioclases and amphiboles exhibit similar trends (Fig. 8). This variation in the slope of the straight lines of CSD diagrams in sheared metabasites is due to the selective elimination of coarsest crystals. Such a process is characteristic of dynamic recrystallisation processes during mylonitization in a ductile shear zone (e.g. Passchier and Trouw, 1996), and important decreases in crystal size have been traditionally interpreted in terms of retrograde metamorphism (e.g. Michibayasi and Masuda, 1993) or mylonitic deformation (e.g. White et al., 1980). Therefore, the observed CSD diagrams are in close agreement with the structural and metamorphic observations in the SISZ.

The slope of the straight line of amphiboles is usually lower than that of the plagioclase for the same sample. This difference is more obvious in samples corresponding to the rocks affected by the SISZ (Fig. 7b). This fact would imply a priori that the crystal size reduction due to mylonitization is more intense in the plagioclase than in the amphibole. However, it is important to remember that in this work CSD diagrams are computed using the long axis intersection length. The habit of amphiboles is short prismatic in the banded amphibolites and long prismatic in the sheared metabasites, whereas plagioclases usually show a rounded or short prismatic habit (Fig. 5a). Therefore, although the crystal size distribution is similar for both plagioclases and amphiboles in each sample, the long axis of the latter is always longer than that of the former. As we enter the SISZ and the habit of amphiboles becomes longer, this difference accentuates. Therefore, differences in the slope of the straight line of amphiboles and plagioclases indicate a change in the shape of amphibole crystals that coincides approximately with a change in their composition, since in the sheared metabasites amphiboles are more actinolitic (Díaz Azpiroz, 2001).

Sudden changes in the CSD plots are observed in Fig. 8 for rocks affected by a high metamorphic grade that were subsequently subjected to a mylonitic deformation under retrograde conditions (Fig. 8). This suggests that CSD plots could be used in the future to discriminate among different tectono-metamorphic events that affected a given rock.

6. Conclusions

The results of the crystal size and shape analysis of the Acebuches metabasites are in agreement with the most important statements made so far about these rocks (Bard, 1969, 1970; Crespo-Blanc, 1991; Castro et al., 1996a; Díaz Azpiroz, 2001). The upper half of the series, and possibly the entire sheet, was affected by a HT/LP metamorphic event (M_1) that gave place to coarse-to-medium-grained banded amphibolites. The estimated metamorphic temperature decreases towards the bottom of the series, defining an inverted metamorphic gradient. Straight lines in CSD diagrams show similar slopes and increasing intercepts with the decrease in the estimated metamorphic temperature (Fig. 9a). This is probably related to differences in nucleation rates or other kinetic factors activated by temperature, and it explains the observed textural transition from coarse-grained (top of the sheet) to medium-grained amphibolites. The lower half of the metabasite sheet was also affected by the retrometamorphism (M_2) and the mylonitization (D_2) associated with the SISZ. The intensity of the deformation in the SISZ increased progressively downwards from the middle levels of the Acebuches. Straight lines in CSD diagrams from samples taken from the SISZ show slopes that increase with the intensity of deformation inside the shear zone (Fig. 9b), a variation that is related to the elimination of crystals with largest sizes by processes of dynamic recrystallization.

In summary, CSD diagrams seem to show characteristic patterns of variation in metamorphic rocks. Differences in temperature of less than 100 °C are enough to imprint significant variations (several orders of magnitude) in the intercept of the straight segments of CSD diagrams. On the other side, an increase in the intensity of mylonitization processes implies steeper straight lines in CSD plots. Therefore, it is suggested that CSD diagrams can be a useful tool to analyse deformation events in medium-to-high grade metamorphic rocks, especially where other structural or metamorphic indicators are scarce or ambiguous. Future improvements of the method should include an analysis of the relationships between the slopes of the CSD straight lines and strain or strain-rate measurements in shear zones.

Acknowledgements

Constructive reviews by Jörn H. Kruhl, Karina Zavala and Dougal A. Jerram greatly improved the manuscript. The results presented in this work are a part of the Ph.D. Thesis of Manuel Díaz Azpiroz. Financial support from project PB94-1085 (Spanish Science Commission, CICYT-DGES) and the University of Huelva is gratefully acknowledged.

References

Armienti, P., Pareschi, M.T., Innocenti, F., Pompilio, M., 1994. Effects of magma storage and ascent on the kinetics of crystal growth. Contributions to Mineralogy and Petrology 115, 402–414.

Bard, J.P., 1969. Le métamorphisme régional progressif de Sierra de Aracena en Andalousie occidentale (Espagne). Ph.D. thesis, University of Montpellier.

Bard, J.P., 1970. Composition of Hornblendes formed during the Hercynian progressive Metamorphism of the Aracena Metamorphic Belt (SW Spain). Contributions to Mineralogy and Petrology 28, 117–134.

Bell, T.H., Etheridge, M.A., 1973. Microstructure of mylonites and their descriptive terminology. Lithos 6, 337–348.

Cashman, K.V., Ferry, J.M., 1988. Crystal size distribution (CSD) in rocks and the kinetics and dynamics of crystallisation. III. Metamorphic crystallisation. Contributions to Mineralogy and Petrology 99, 401–415.

Cashman, K.V., Marsh, B.D., 1988. Crystal size distribution (CSD) in rocks and the kinetics and dynamics of crystallisation. II. Makaopuhi lava lake. Contributions to Mineralogy and Petrology 99, 292–305.

Castro, A., Fernández, C., de la Rosa, J.D., Moreno-Ventas, I., Rogers, G., 1996a. Significance of MORB-derived amphiboles from the Aracena Metamorphic Belt, Southwest Spain. Journal of Petrology 37, 235–260.

Castro, A., Fernández, C., de la Rosa, J.D., Moreno-Ventas, I., El-Hmidi, H., El-Biad, M., Bergamín, J.F., Sánchez, N., 1996b. Triple-junction migration during Paleozoic plate convergence: the Aracena metamorphic belt, Hercynian massif, Spain. Geologische Rundschau 85, 180–185.

Castro, A., Fernández, C., El-Hmidi, H., El-Biad, M., Díaz, M., de la Rosa, J.D., Stuart, F., 1999. Age constraints to the relationships between magmatism, metamorphism and tectonism in the Aracena metamorphic belt, southern Spain. Geologische Rundschau 88, 26–37.

Crespo-Blanc, A., 1991. Evolución geotectónica del contacto entre la zona de Ossa–Morena y la zona Surportuguesa en las sierras de Aracena y Aroche (Macizo Ibérico Meridional): Un contacto mayor en la cadena Hercínica Europea. Ph.D. thesis, University of Sevilla.

Crespo-Blanc, A., Orozco, M., 1988. The Southern Iberian Shear Zone: a major boundary in the Hercynian folded belt. Tectonophysics 148, 221–227.

Díaz Azpiroz, M., 2001. Evolución tectono-metamórfica del dominio de alto grado de la banda metamórfica de Aracena. Ph.D. thesis, University of Huelva.

Dupuy, C., Dostal, J., Bard, J.P., 1979. Trace element geochemistry of paleozoic amphibolites from SW Spain. Tschermaks Mineralogische und Petrographische Mitteilungen 26, 87–93.

Eberl, D.D., Srodon, J., Kralik, M., Taylor, B.E., Peterman, Z.E., 1990. Ostwald ripening of clays and metamorphic minerals. Science 248, 474–477.

Eden, C., 1991. Tectonostratigraphic analysis of the northern extent of the oceanic exotic terrane, northwestern Huelva province, Spain. Ph.D. thesis, University of Southampton.

El-Biad, M., 2000. Generación de granitoides en ambiente geológicamente contrastados del Macizo Ibérico. Limitaciones experimentales entre 2 y 15 kbar. Ph.D. thesis, University of Huelva.

El-Hmidi, H., 2000. Petrología y geoquímica de los sistemas andesíticos ricos en Mg: estudio petrológico y experimental de las noritas de la Banda Metamórfica de Aracena, SO de España. Ph.D. thesis, University of Huelva.

Ernst, W.G., Liou, J., 1998. Experimental phase equilibrium study of Al- and Ti-contents of calcic amphibole in MORB—a semiquantitative thermobarometer. American Mineralogist 83, 952–969.

Galwey, A.K., Jones, K.A., 1966. Crystal size frequency distribution of garnets in some analysed metamorphic rocks from Mallaig, Inverness, Scotland. Geological Magazine 103, 143–152.

Ghiorso, M.S., 1987. Chemical mass transfer in magmatic processes, III. Crystal growth, chemical diffusion and thermal diffusion in multicomponent magmatic melts. Contributions to Mineralogy and Petrology 96, 291–313.

Higgins, M.D., 1994. Numerical modelling of crystal shapes in thin sections: estimation of crystal habit and true size. American Mineralogist 79, 113–119.

Higgins, M.D., 1996. Crystal size distributions and other quantitative textural measurements in lavas and tuffs from Egmont volcano (Mt. Taranaki), New Zealand. Bulletin of Volcanology 58, 194–204.

Higgins, M.D., 2000. Measurement of crystal size distributions. American Mineralogist 85, 1105–1116.

Holland, T.J.B., Blundy, J.D., 1994. Non-ideal interactions in calcic amphiboles and their bearing on amphibole–plagioclase thermometry. Contributions to Mineralogy and Petrology 116, 433–447.

Jerrall, D.A., 2001. Visual comparators for degree of grain-size sorting in two and three-dimensions. Computers and Geoscience 27, 485–492.

Jones, K.A., Galwey, A.K., 1966. Size distribution, composition and growth kinetics of garnet crystals of some metamorphic rocks from west of Ireland. Journal Geological Society of London 122, 29–44.

Jones, K.A., Morgan, G.J., Galwey, A.K., 1972. The significance of the size distribution function of crystals formed in metamorphic reactions. Chemical Geology 9, 137–143.

Kirkpatrick, R.J., 1977. Nucleation and growth of plagioclase, Makaopuhi and Alae lava lakes, Kilauea Volcano, Hawaii. Geological Society of America Bulletin 88, 78–84.

Kretz, R., 1966. Grain-size distribution for certain metamorphic minerals in relation to nucleation and growth. Journal of Geology 74, 147–173.

Maaløe, S., Tumyr, O., James, D., 1989. Population density and zoning of olivine phenocrysts in tholeiites from Kauai, Hawaii. Contributions to Mineralogy and Petrology 101, 176–186.

Marsh, B.D., 1988. Crystal size distribution (CSD) in rocks and the kinetics and dynamics of crystallisation. Contributions to Mineralogy and Petrology 99, 277–291.

Marsh, B.D., 1998. On the interpretation of crystal size distributions in magmatic systems. Journal of Petrology 39, 553–599.

Means, W.D., 1981. The concept of steady-state foliation. Tectonophysics 78, 179–199.

Michibayasi, K., 1993. Syntectonic development of a strain-independent steady-state grain size during mylonitization. Tectonophysics 222, 151–164.

Michibayasi, K., Masuda, T., 1993. Shearing during progressive retrogression in granitoids: abrupt grain size reduction of quartz at the plastic–brittle transition for feldspar. Journal of Structural Geology 15, 1421–1432.

Munhá, J.M., Oliveira, J.T., Ribeiro, A., Oliveira, V., Quesada, C., Kerrich, R., 1986. Beja–Acebuches ophiolite: characterisation and geodynamic significance. Maleo 2, 30.

Passchier, C.W., Trouw, R.A.J., 1996. Microtectonics, Springer-Verlag, Berlin.

Peacock, S.M., 1987. Creation and preservation of subduction-related inverted metamorphic gradients. Journal of Geophysical Research 92, 12763–12781.

Peterson, T.D., 1990. Petrology and genesis of natrocarbonatite. Contributions to Mineralogy and Petrology 105, 143–155.

Peterson, T.D., 1996. A refined technique for measuring crystal size distributions in thin section. Contributions to Mineralogy and Petrology 124, 395–405.

Quesada, C., Fonseca, P.E., Munhá, J., Oliveira, J.T., Ribeiro, A., 1994. The Beja–Acebuches Ophiolite (Southern Iberia Variscan fold belt): geological characterization and geodynamic significance. Boletín Geológico y Minero de España 105, 3–49.

Ranalli, G., 1984. Grain size distribution and flow stress in tectonites. Journal of Structural Geology 6, 443–447.

Randolph, A.D., Larson, M.A., 1971. Theory of Particulate Processes, Academic Press, New York.

Ree, J.-H., 1991. An experimental steady-state foliation. Journal of Structural Geology 13, 1001–1011.

Shelley, D., 1993. Igneous and Metamorphic Rocks under the Microscope, Chapman and Hall, London.

Sibson, R.H., 1977. Faults rocks and fault mechanisms. Journal of the Geological Society (London) 133, 191–213.

Tullis, J., Yund, R.A., 1985. Dynamic recrystallisation of feldspar: a mechanism for ductile shear zone formation. Geology 13, 238–241.

White, S.H., Burrows, S.E., Carreras, J., Shaw, N.D., Humphreys, F.J., 1980. On mylonites in ductile shear zones. Journal of Structural Geology 2, 175–187.

Wilhelm, S., Wörner, G., 1996. Crystal size distribution in Jurassic Ferrar flows and sills (Victoria Land, Antartica): evidence for processes of cooling, nucleation and crystallisation. Contributions to Mineralogy and Petrology 125, 1–15.